Research of a wind tunnel parameters by means of cross-section analysis of air flow profiles

Vitalii Yanovych, Daniel Duda, Vít Horáček, et al.

View Online   Export Citation

ARTICLES YOU MAY BE INTERESTED IN

Research of a Wind Tunnel Parameters by Means of Cross-Section Analysis of Air Flow Profiles

Vitalii Yanovych[1, a)], Daniel Duda[1, b)], Vít Horáček[1, c)] and Václav Uruba[1, 2, d)]

^{1}*Department of Power System Engineering, Faculty of Mechanical Engineering, University of West Bohemia in Pilsen, Univerzitní 22, 306 14 Pilsen, Czech Republic.*
^{2}*Department of Power System Engineering, Institute of Thermomechanics, Czech Academy of Sciences, Dolejškova 5, 182 00, Prague, Czech Republic.*

a)Corresponding author: yanovichvitaliy@i.ua
b)dudad@kke.zcu.cz
c)vhoracek@students.zcu.cz
d)uruba@kke.zcu.cz.

Abstract. Wind tunnel is constructed. It is characterized by a high degree of airflow laminarization. The main constructive element of this aerodynamic tube is the laminarization module. It allows the destruction of turbulent fluxes by providing a homogeneous laminar flow. In order to evaluate the performance of the developed aerodynamic tube, a series of experimental studies was conducted in the range of air velocity of 10-50 m·s^{-1}. To establish the laws of the distribution of flow parameters relative to the section the cross-sectional analysis method was used. It consists of forming a series of measuring planes that characterize the distribution of dynamic pressure and air flow velocity relative to the testing section. After that, the received experimental data are interpreted as three-dimensional graphic dependencies of the studied quantities. There is clearly observed a certain local area of stable values of dynamic pressure and flow velocity, after which they are sharply reduced in the direction of the walls of the section for testing. As a result of the analysis, a series of digital profiles of the distribution of dynamic pressure in the measuring planes of the testing section were obtained. Analysis of the obtained graphic dependencies allowed establishing of the uneven distribution of the dynamic pressure difference in the boundary layer zone along the inner perimeter of the test section is worth noting. Because of the side of the upper wall of the test section, the dynamic pressure difference is greater than the sidewall. This phenomenon is due to the difference in area of their blown air. Consequently, at a wall with a larger contact surface, a constant air stream experiences more loss of its kinetic energy than a wall with a smaller area. Especially this tendency is observed in the turbulent boundary layer.

INTRODUCTION

The separation of the flow from the overflown surface of the body accompanies most gas flows at certain Reynolds numbers. For the first time a rational explanation of this phenomenon was given by Prandtl in [1], which laid the foundation of the theory of the boundary layer.

According to the Prandtl theory, separation from the smooth surface of a solid at large Reynolds numbers occurs as a result of a decrease in velocity at the outer boundary of a thin wall viscous boundary layer and is accompanied by vanishing at some point of surface friction [2-5]. Behind this point is the area of return currents. The distribution of velocity and pressure on the outer boundary of the boundary layer is determined by solving the external problem of the flow of an ideal fluid around a body.

The idea of the interaction of the boundary layer with the external non-viscous flow formed the basis of the theory created in 1969 by Neyland [6] and independently by Stewartson and Williams [7]. At the same time, they considered the problem of separation of the boundary layer from a flat surface of a gas stream with large Reynolds numbers and applied the same approach to its solution - flow analysis in the vicinity of the separation point was

performed by constructing an asymptotic solution of the Navier – Stokes equations as the Reynolds number tends to infinity.

In this case, the method of matched asymptotic expansions [8], [9], [10] was used, which has received widespread in recent years not only in the theory of a collapsing boundary layer, but also in other sections of theoretical aerodynamics.

The modern diversity of methods research of the boundary layer does not give a clear idea of the source theory of the appearance and propagation of the boundary layer around the surface of the body [10-12]. To date, there is an urgent task, the search for new methods for determining the characteristics of the air flow near the overflown surface.

DESCRIPTION OF EXPERIMENTAL EQUIPMENT

In the laboratory of the Department of Power Machines of the University of West Bohemia in Pilsen, the Czech Republic, in collaboration with WTTech.CZ, an open tunnel aerodynamic tunnel was developed (Fig. 1). The uniqueness of this tunnel is its ability to homogenize the turbulent flow, which leads to the formation of a high laminar flow of air. The speed of this flow can be 0-80 m·s⁻¹.
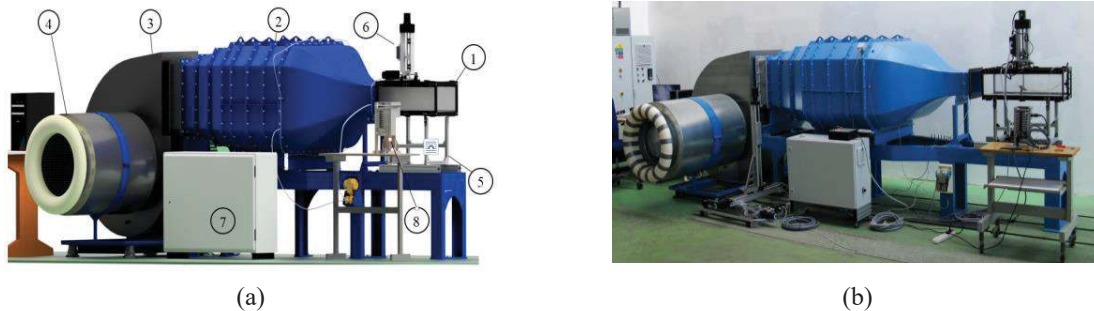

| (a) | (b) |

FIGURE 1. Experimental model of the wind tunnel and equipment for its research. (a) 3D model of wind tunnel, (b) implementation of the tunnel, (1) test section, (2) a module for air flow laminarization, (3) ventilator, (4) air filter, (5) frame, (6) 2D traverse, (7) the switching block of the traverse, (8) pressure analysis system.

The tunnel contains a closed-loop measuring chamber with a measuring section of 300×200 mm, the length of the chamber is 740 mm. Its side walls are made of extruded polycarbonate with high surface quality and optical purity. The side walls and the bottom of the measuring chamber are made of a monoblock. The top wall is modular and allows you to combine parts of the upper cover of the measuring chamber with auxiliary equipment, according to the necessity of the experiment (Fig. 2).
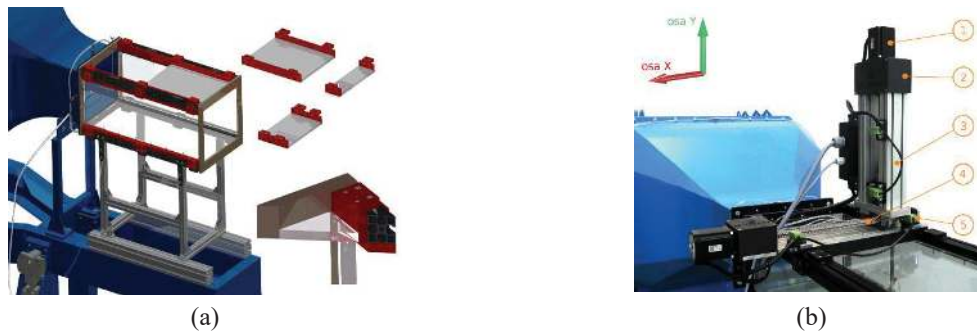

| (a) | (b) |

FIGURE 2. Convergence of the measuring chamber design. (a) 3D model of the measuring chamber, (b) placement of a set of nozzles for finding static pressure in the chamber and placement of a two-coordinate traverse in the chamber's measuring space, (1) stepper motor; (2) clamping guides; (3) guides; (4) ball screw; (5) limiters.

In the upper right part of Fig. 2 a, individual modular elements of the upper wall are displayed, the installation or disassembly of which allows the upper part of the measuring space to be adjusted for measuring equipment, for example, a set of nozzles for finding a static pressure and the placement of a two-coordinate traverse 2 (b).

The main constructive element of the developed tunnel is the laminarisation unit of the air flow, which consists of a diffuser, a camera for laminarisation air streams and an the initial nozzle which combines with a measuring chamber. The purpose of the laminar camera is to destroy vortices that turbulize the air flow.
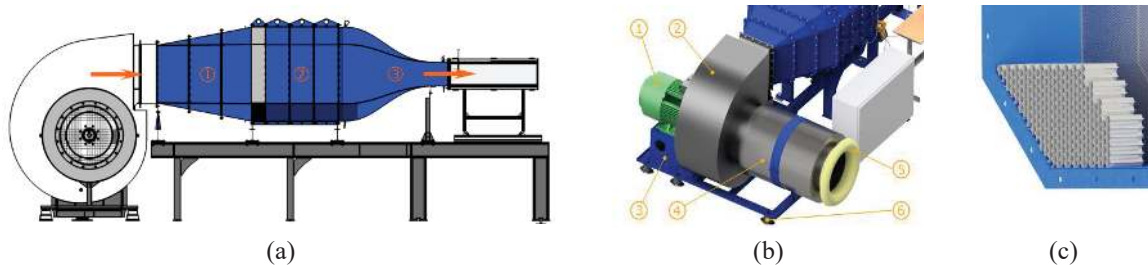

| (a) | (b) | (c) |

FIGURE 3. Principal scheme of the aerodynamic tunnel. (a) The principle of work, (b) flow generation system, (c) honeycomb straightener, (1) diffuser, (2) laminar camera, (3) the initial nozzle.

The air is fed by the fan to the diffuser. As a result of the difference between the input and output plane of the diffuser, the velocity decreases. Lowering the flow rate is advantageous in terms of pressure loss for its further passage through the laminarization unit. The diffuser has a rectangular input of 400×500 mm and a rectangular output of 1150×800 mm with slanted angles of $15°$ and a chamfer of $150 \times 45°$. The diffuser tilt is designed to avoid unwanted secondary airflow. The length of the diffuser is 800 mm and is divided into three sections. Each section is a steel welding case. Between parts of this case, there are metal grids for pre-treatment of the fluid. To prevent vibration transmission from the fan, the diffuser is connected with a flexible coupling.

The laminarization unit has a section of 740 mm. The cross-sectional dimension corresponds to the diffuser output. The purpose of this module is to level the turbulence of the stream, due to the destruction of air vortices, which determine the momentum of the flow velocity. For this purpose, the camera space is divided into four separate sections. Between them are installed metal screens. Each section is a steel body and allows extracting pressure at two points - in the upper and lower parts of the camera.

In order to avoid the unfolding of the flow along its axis in the first section of the module, an additional element, in the form of a hexagonal membrane, is installed. In the last part of the laminarization module there is a thermometer measuring the temperature of the flowing environment.

After the laminarization module there is a confuser, which is designed to accelerate the flow of air. From a structural point of view, it is a metal construction with complex configurations, which ends with a corresponding outlet for the measuring chamber. The length of the diffuser is 920 mm. At the inlet and outlet of this confuser, 4 static pressure vents are located, which allow measuring the flow rate through the tunnel. Inlet openings of static pressure are symmetrically located in the middle of all four cones of the diffuser.

The radial-type ZVVZ aerodynamic tube fan is powered by a three-phase Tamel electric motor with a maximum output of 55 kW and a shaft rotation speed of 2955 per minute. The capacity used by the tunnel is 45.7 kW at 2270 rpm.

The air is taken through a cylindrical filter that prevents the entry of unwanted objects to the tunnel.

To determine the operational characteristics of the aerodynamic tunnel, a special probe was developed. Which contains four eccentrically placed Pitot tubes. The distance between the tubes is 70 mm, the outer diameter of the tube is 2 mm, the diameter of the tube opening is 1.6 mm, the length is 55 mm. The design of the probe provides measurement of the profile of the dynamic pressure, the air flow velocity and the magnitude of its boundary layer throughout the measuring plane of the test section. The motion of the developed probe is accomplished by moving the two-coordinate traverse. The transmission of the received pressure is carried out at the expense of the pneumatic highway, which connects to the collector and goes to the pressure measurement system.

The pressure measurement system is a set of several Chell Instruments modules from the Net Scanner series. The main module is the Net Scanner Model 9116 pressure sensor. This model is a sixteen-channel sensor capable of measuring the pressure of dry gases. Individual channels do not depend on each other and include piezo-resistor pressure sensors with a wide range of measurements.

Data from individual channels are evaluated using an integrated 32-bit microprocessor that allows you to compensate for temperature errors. All sensors have their own user memory to accurately calibrate each channel. The accuracy of this device is ± 0.05%. The connection to other equipment is via an Ethernet cable. This device acts as a relative, that is, as a result of its operation, the difference between the total and the static pressure values is generated. As a result, we obtain the values of dynamic pressures from each digital channel of the device.

SOFTWARE FOR DATA ANALYSIS

For the visualization of the profiles of the measuring variables and their subsequent analysis, a recombination algorithm with corrective function was developed. The idea of it is to analyze the sector and averaged the data of the common areas of the measuring plane.

On the basis of the developed algorithm in the program environment LabVIEW was developed a program for graphical interpretation of the data provided they are parallel decoding (Fig. 4).
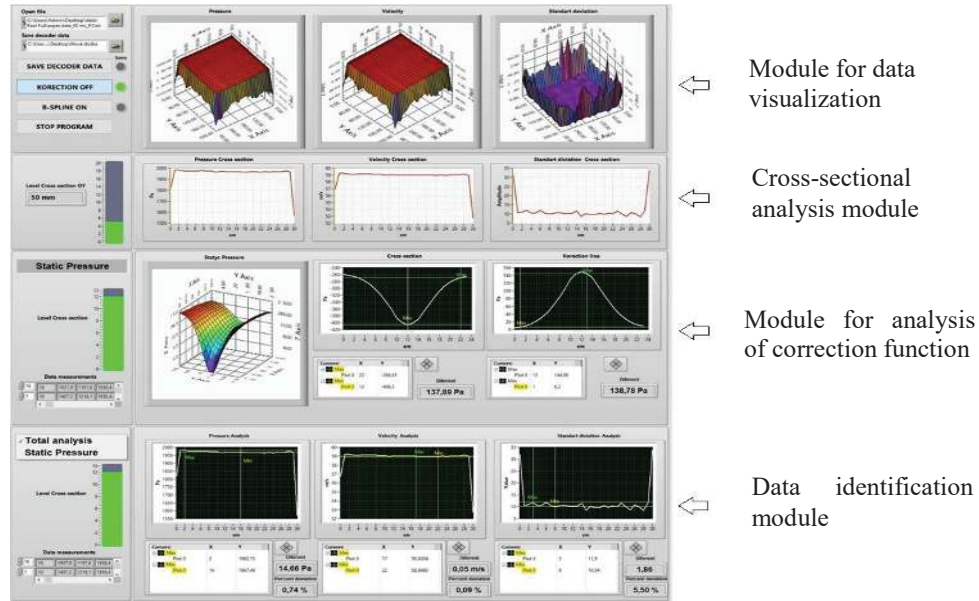

Module for data visualization

Cross-sectional analysis module

Module for analysis of correction function

Data identification module

FIGURE 4. Program interface for data analysis.

In addition, the functionality of the program allows you to analyze the data obtained, depending on the type of their numerical recombination. The first type is the display of data, taking into account the corrective function. The second type is the display of data taking into account the function of B-Spline. It is used to fit the curve and the numerical differentiation of experimental data. The third type is the display of the original decoding data without taking into account the corrective functions

CROSS-SECTIONAL ANALYSIS OF THE RESULTS OF EXPERIMENTAL RESEARCH

In order to evaluate the performance of the developed aerodynamic tube, a series of experimental studies was conducted in the range of air velocity of 10-50 m·s^{-1}. The research was carried out in three measuring planes of the testing section. The first plane S_1 was located at a distance of 38 mm from the inlet of the test section, the second plane S_2 at a distance of 225 mm, the third plane S_3 at a distance of 595 mm. As a result of the experimental data obtained, a series of cross-sectional profiles of dynamic pressure was formed in the measuring planes, depending on the change in air flow velocity (Fig. 5).

Each cross-sectional profile consisted of 650 experimental points. The interval between which varied from 2 to 10 mm, depending on the study area of the measuring plane. For the study area, which was up to 8 mm from the walls of the test section, the measurement interval was 2 mm, while the interval between other points was 10 mm.
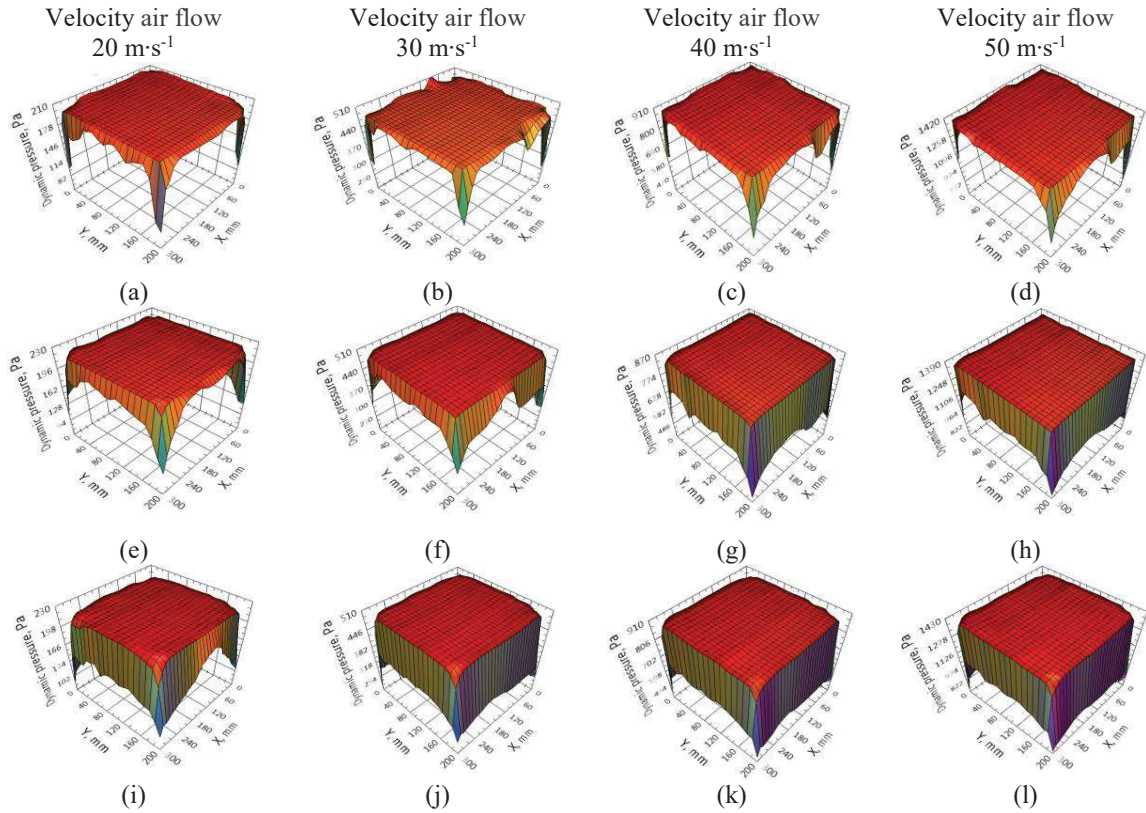
| Velocity air flow 20 m·s⁻¹ | Velocity air flow 30 m·s⁻¹ | Velocity air flow 40 m·s⁻¹ | Velocity air flow 50 m·s⁻¹ |

(a) (b) (c) (d)

(e) (f) (g) (h)

(i) (j) (k) (l)

FIGURE 5. Dynamic pressure profiles, depending on the position of the measuring area and the speed of the flow stream. (a), (b), (c), (d) Dynamic pressure in plane S_1. (e), (f), (g), (h) Dynamic pressure in planes S_2. (i), (j), (k), (l) Dynamic pressure in plane S_3. X, Y the axes of the test section.

On the graphs, it is clearly observed some local area of stable values of dynamic pressure, after which it is sharply reduced in the direction of the walls of the section for testing. That is, the section of the boundary layer begins. The value of the dynamic pressure (Pd) prior to the beginning of the boundary layer varies depending on the air flow velocity and has a range of values for $V = 10$ m·s⁻¹ - Pd = 54-60 Pa, $V = 20$ m·s⁻¹ - Pd = 200-215 Pa, for $V = 30$ m·s⁻¹ - Pd = 475-495 Pa, for $V = 40$ m·s⁻¹ - Pd = 860-877 Pa, for $V = 50$ m·s⁻¹ - Pd = 1365-1383 Pa. The presence of a range of values of dynamic pressure is due to the fact that, depending on the position of the measuring section in the direction of increasing the distance from the input of the camera for testing and increasing the speed of the wind flow, there is an increase in the dynamic pressure.
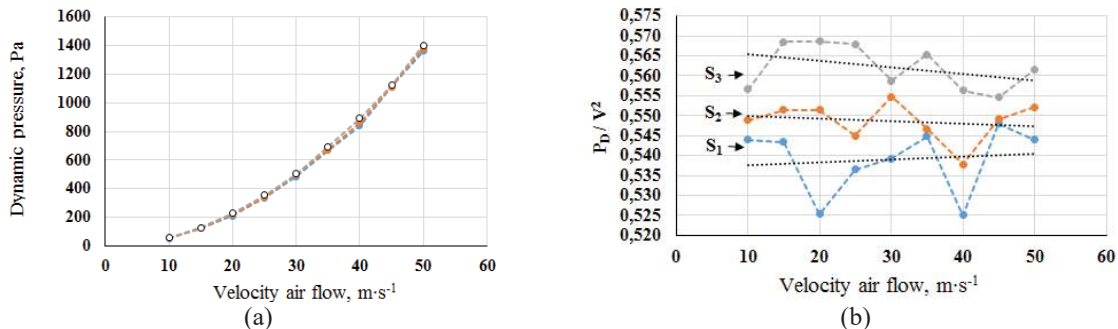

(a)   (b)

FIGURE 6. Distribution of dynamic pressure depending on the air flow velocity (a) and its normalized distribution (b).

This graphic dependence shows the exponential character of the distribution of the value of the dynamic pressure relative to the flow velocity.

The analysis of the experimental data obtained allowed establishing the regularity of the change in the dynamic pressure of the depending on the airflow velocity (Fig. 6).

As a result of experimental studies, a series of flow graphic flow profiles was obtained depending on the location of the measuring plane (Fig. 7). The analysis of the obtained dependences showed the identical character of the graphical distribution of the received data as in the case of dynamic pressure.

Based on the experimental data, the distribution of airflow velocity and dynamic pressure, depending on the location of the measuring section. Also taking into account the classical assertion that the dynamic pressure, and as a consequence, and the speed of the air stream, sharply decreases when the sections close to the walls are tested. We received a series of digital profiles of the distribution of dynamic pressure in the measuring planes of the test section, in particular at its corners (Fig. 8). The analysis of the graphic dependences obtained allowed establishing the thickness of the boundary layer of the flow.
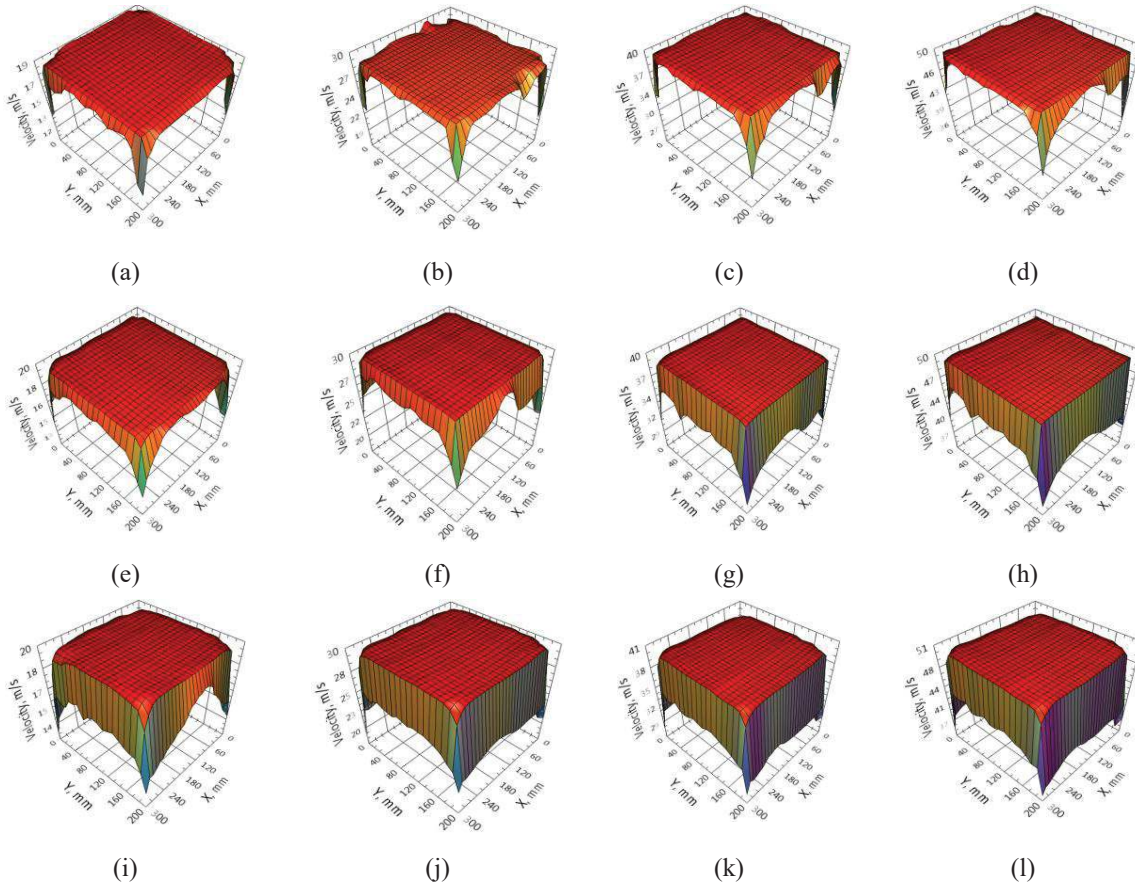

| (a) | (b) | (c) | (d) |

| (e) | (f) | (g) | (h) |

| (i) | (j) | (k) | (l) |

FIGURE 7. Profiles of the speed of the flow depending on the positions of the measuring plane. (a), (b), (c), (d) is the flow rate in plane S_1. (e), (f), (g), (h), is the flow rate in plane S_2. (i), (j), (k), (l) is the flow rate in plane S_3. X, Y the axes of the test section.

As we can see from Fig. 8, with increasing distance in the direction of the exit of the section for testing, there is a sharp increase in the boundary layer of the flow. Moreover, on the received digital profiles, there are clearly three main dynamic pressure changes zones.

The first zone characterizes the diffusion part of the boundary layer of the stream and contains the lowest values of dynamic pressure. The second zone characterizes the dynamic part of the boundary layer. The third zone is a section of stable values of dynamic airflow pressure. An especially sharp increase in the difference in the dynamic pressure is observed in the measuring plane S_3 whereas in the measuring plane S_1 and S_2, the distribution of the

dynamic pressure is almost the same. It is also worth noting that in the digital profile of the measuring section S_3 (Fig. 8 c), unlike S_1, (Fig. 8 a) and S_2 (Fig. 8 b), near the corners of the camera for testing, there is a certain rounding of the boundary flow layer.

This analysis allows us to conclude that in the measuring section S_3 the boundary layer of the airflow is turbulent. Also, analysis of the obtained graphic dependencies allowed establishing of the uneven distribution of the dynamic pressure difference in the boundary layer zone along the inner perimeter of the test section is worth noting. Because of the side of the upper wall of the test section, the dynamic pressure difference is greater than the sidewall. This phenomenon is due to the difference in area of their blown air. Consequently, at a wall with a larger contact surface, a constant air stream experiences more loss of its kinetic energy than a wall with a smaller area. Especially this tendency is observed in the turbulent boundary layer.
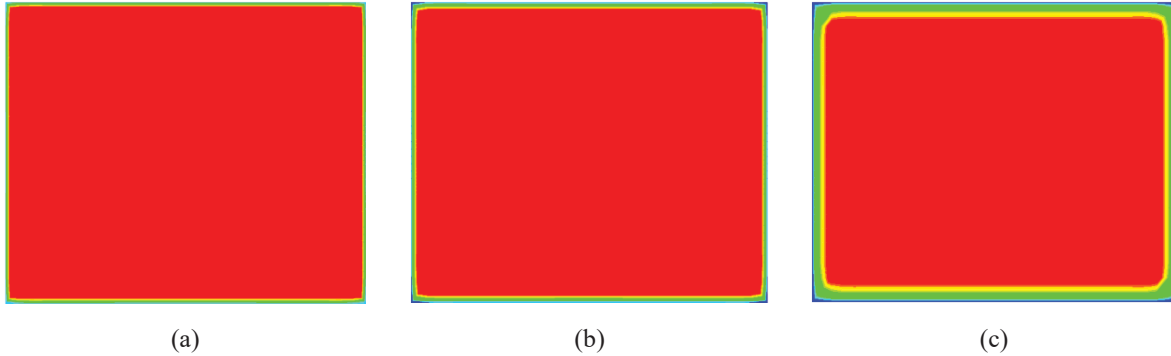

(a)	(b)	(c)

FIGURE 8. The distribution of the dynamic pressure in the measuring planes of the section for testing at an air flow velocity of 50 m·s^{-1} depending on the position of the measuring plane in the testing section, (a) position of the measuring plane S_1, (b) position of the measuring plane S_2, (c) position of the measuring plane S_3.

CONCLUSION

The performance evaluation of the developed aerodynamic tunnel was performed on the basis of cross-sectoral analysis of the measuring planes of the test section. As a result of the experimental studies, a series of graphical profiles of flow velocity and dynamic pressure were obtained, depending on the location of the measuring plane. The analysis of the obtained data allowed to establish the change in the dynamic pressure depending on the position of the measuring section.

The visual interpretation of the obtained data leads to the conclusion that the developed aerodynamic tunnel has a high degree of laminarisation of the air flow.

ACKNOWLEDGMENTS

REFERENCES

1. L. Prandtl, Ubr "Flussigkeitsbewegung bei sehr Kleiner Reibung", Verh. d. 3 Int. Math.-Kongr., Heilderberg, Leipzig: Teubner, 484-491 (1905).
2. L. Howarth, "On the solution of the laminar boundary layer equations", Proc. Roy. Soc. London, 164(919), 547-579 (1938).
3. S. Goldstein, "On laminar boundary-layer flow near position of separation" Quart. J. Mech. Appl. Math., 1(1), 43-69 (1948).
4. J. Ackeret, F. Feldman and N. Rott, "Investigation of compression shocks and boundary layers in gases moving at high speed". NACA Tech. Note 1113, 1947.

5. H.W. Liepmann, "The interaction between boundary layers and shock waves in transonic flow". J. Aeronaut. Sci., 13(12), 623-637 (1946).
6. K. Stewartson and P.G. Williams, "Self-induced separation", Proc. Roy. Soc. London, 312(1509), 181-206 (1969).
7. M.D. Van Dyke, "Perturbation methods in fluid mechanics", New York: Academic Press, 1964.
8. J.D. Cole, "Perturbation methods in applied mathematics" Waltham (Mass.): Blaisdell Publ. Co., 1968.
9. P.A. Lagerstrom and R.G. Casten, "Basic concepts underlying singular perturbations techniques", SIAM Rev., 14(1), 163-120 (1972).
10. V. Uruba, "Decomposition methods in turbulence research", EPJ Web of Conferences 25, 01095, (2012).
11. V. Uruba, "On aerodynamic forces physical mechanism", AIP Conference Proceedings 1768(1), 020011 (2016).
12. O. Hladík and V. Uruba, "Analysis of intermittent signal", Mechanical Engineering J., June 2009, 69-70 (2009).